American Physiological Society | Journal of Applied Physiology

PUBLISHED ARTICLE
ARCHIVES
SUBSCRIPTIONS
SUBMISSIONS
CONTACT US

J Appl Physiol (1985). 2019 Apr 1; 126(4): 854–862.
Published online 2019 Jan 3.
doi: 10.1152/japplphysiol.00838.2018: 10.1152/japplphysiol.00838.2018

PMCID: PMC6485689
PMID: 30605400

Sustained Klotho delivery reduces serum phosphate in a model of diabetic nephropathy

Julia M. Hum,[1,2,*] Linda M. O'Bryan,[3,*] Arun K. Tatiparthi,[4] Erica L. Clinkenbeard,[1] Pu Ni,[1] Martin S. Cramer,[3] Manoj Bhaskaran,[5] Robert L. Johnson,[5] Jonathan M. Wilson,[6] Rosamund C. Smith,[3] and Kenneth E. White[✉1]

[1]Division of Molecular Genetics and Gene Therapy, Department of Medical and Molecular Genetics, Indiana University School of Medicine, Indianapolis, Indiana
[2]Division of Biomedical Sciences, College of Osteopathic Medicine, Marian University, Indianapolis, Indiana
[3]Biotechnology Discovery Research, Lilly Research Laboratories, Eli Lilly and Company, Indianapolis, Indiana
[4]Lead Optimization Toxicology and Pharmacology, Covance Incorporated, Greenfield, Indiana
[5]Toxicology and Pathology, Eli Lilly and Company, Indianapolis, Indiana
[6]Tailored Therapeutics, Eli Lilly and Company, Indianapolis, Indiana
[✉]Corresponding author.
* J. M. Hum and L. M. O'Bryan are co-first authors on this work.
Address for reprint requests and other correspondence: K. E. White, Dept. of Medical and Molecular Genetics, Indiana Univ. School of Medicine, 975 W. Walnut St., IB130, Indianapolis, IN 46202 (e-mail: kenewhit@iupui.edu).

Received 2018 Sep 21; Revised 2018 Dec 12; Accepted 2018 Dec 29.

Abstract

Diabetic nephropathy (DN) is a primary cause of end-stage renal disease and is becoming more prevalent because of the global rise in type 2 diabetes. A model of DN, the *db/db* uninephrectomized (*db/db*-uni) mouse, is characterized by obesity, as well as compromised renal function. This model also manifests defects in mineral metabolism common in DN, including hyperphosphatemia, which leads to severe endocrine disease. The FGF23 coreceptor, α-Klotho, circulates as a soluble, cleaved form (cKL) and may directly influence phosphate handling. Our study sought to test the effects of cKL on mineral metabolism in *db/db*-uni mice. Mice were placed into either mild or moderate disease groups on the basis of the albumin-to-creatinine ratio (ACR). Body weights of *db/db*-uni mice were significantly greater across the study compared with lean controls regardless of disease severity. Adeno-associated cKL administration was associated with increased serum Klotho, intact, bioactive FGF23 (iFGF23), and COOH-terminal fragments of FGF23 ($P < 0.05$). Blood urea nitrogen was improved after cKL administration, and cKL corrected hyperphosphatemia in the high- and low-ACR *db/db*-uni groups. Interestingly, 2 wk after cKL delivery, blood glucose levels were significantly reduced in *db/db*-uni mice with high ACR ($P < 0.05$). Interestingly, several genes associated with stabilizing active iFGF23 were also increased in the osteoblastic UMR-106 cell line with cKL treatment. In summary, delivery of cKL to a model of DN normalized blood phosphate levels regardless of disease severity, supporting the concept that targeting cKL-affected pathways could provide future therapeutic avenues in DN.

NEW & NOTEWORTHY In this work, systemic and continuous delivery of the "soluble" or "cleaved" form of the FGF23 coreceptor α-Klotho (cKL) via adeno-associated virus to a rodent model of diabetic nephropathy (DN), the *db/db* uninephrectomized mouse, normalized blood phosphate levels regardless of disease severity. This work supports the concept that targeting cKL-affected pathways could provide future therapeutic avenues for the severe mineral metabolism defects associated with DN.

Keywords: cKL, diabetes, FGF23, Klotho, phosphate

INTRODUCTION

Diabetes is currently the greatest risk factor for developing chronic kidney disease (CKD), affecting >40% of patients with diabetes (60). The *db/db* mouse line is a genetic obese hyperinsulinemic model of diabetes that develops renal abnormalities similar to patients with type 2 diabetes (67). The *db* gene encodes a G > T point mutation in the leptin receptor that alters hypothalamic responses, causing obesity, hyperlipidemia, hyperinsulinemia, insulin resistance, and diabetes (9, 43). Performing uninephrectomies on *db/db* mice accelerates the progression of diabetic nephropathy (DN) by increasing the strain on the remaining diabetic kidney (29), with a 70% increase in mesangial thickening (6). Nephrectomies at earlier ages of *db/db* mice (6–10 wk) result in profound renal defects by 20–24 wk of age. Typically, a *db/db* mouse uninephrectomized at 6 wk of age will exhibit an increase in albumin-to-creatinine ratio (ACR; 56, 57) by 8 wk of age and a decrease in glomerular filtration rate by 24 wk of age (21, 55). Testing therapeutic interventions in this model of accelerated DN has been useful, particularly in the area of pharmacological inhibitor development for treating renal injury (29, 55, 71).

DN is also associated with development of chronic kidney disease-mineral bone disorder (CKD-MBD; 2, 22). CKD-MBD is clinically characterized in stages of declining kidney function with severe endocrine bone disease, as well as elevated serum parathyroid hormone and bioactive "intact" fibroblast growth factor 23 (iFGF23; 51, 54). CKD-MBD disrupts the normal bone-kidney endocrine axis responsible for regulating mineral metabolism, and hyperphosphatemia develops in late-stage disease (48, 51). In healthy individuals the hormone FGF23, primarily produced by bone, and α-Klotho (α-KL) aid in maintaining normal phosphate and vitamin D homeostasis (40, 41, 45, 72). It is thought that, in part, the hyperphosphatemia due to loss of renal function in CKD leads to increased production of FGF23 (31, 42). Although FGF23 compensates temporarily to maintain normal serum phosphate, with loss of renal mass a decrease in α-KL expression is observed (39). This setting likely leads to "FGF23 resistance" and marked rises in serum phosphate (52).

Two main forms of α-KL protein exist: a full-length transmembrane isoform (mKL; 135 kDa), primarily found in the kidney and parathyroid gland, and a circulating soluble form (cKL; 110 kDa) that can be detected in blood, urine, and cerebrospinal fluid (40). FGF23 initiates signaling through an assembly of mKL coreceptor complexed with FGF receptors (FGFRs), leading to activation of the MAPK cascade (24, 41, 44, 58, 72). The cKL polypeptide, composed of KL1 and KL2 extracellular domains, is generated from cleavage of mKL via activity of the disintegrin and metalloproteinase domain-containing protein-10/17 (ADAM10/17) and β-secretase 1 (BACE) cell surface proteases (49). Prior studies have shown the capability of cKL, in coordination with FGF23, to reduce serum phosphate in normal rodents and the hyperphosphatemic KL-null mouse (30, 68).

Circulating iFGF23 concentrations are regulated by intracellular furin-mediated protease cleavage of FGF23 (70, 73), with polypeptide *N*-acetylgalactosaminyltransferase 3 (GALNT3)-mediated *O*-glycosylation activity protecting iFGF23 (4, 37) and extracellular serine/threonine protein kinase FAM20C (FAM20C) kinase activity destabilizing iFGF23 (70). These changes can be detected in blood by measuring COOH-terminal fragments of FGF23, or cFGF23, by ELISA (35, 74). The posttranslational regulation of mature FGF23 is critical for regulating serum iFGF23 concentrations, as metabolic challenges

such as anemia and hypoxia result in markedly elevated FGF23 mRNA but normal iFGF23 elevated cFGF23 due to proteolysis, to maintain proper phosphate handling in rodents (10, 16) and in humans (7, 32, 61, 63). Importantly, during CKD and with other genetic changes, including inactivating mutations in phosphate-regulating gene with homology to peptidases on the X chromosome (PHEX) and dentin matrix protein-1 (DMP1), resulting in X-linked hypophosphatemia and autosomal recessive hypophosphatemic rickets type 1, respectively, causes "inappropriate" overproduction of iFGF23 (3, 12, 13, 33, 35, 47, 62, 75). The mechanisms responsible for maintaining high iFGF23 are not clear. Herein, we sought to test stable delivery of cKL in a model of DN with mild or moderate degrees of kidney disease and effects on manifestations of CKD-MBD. With sustained cKL delivery to *db/db*-uni mice, blood urea nitrogen (BUN) was partially corrected in moderately severe CKD, and hyperphosphatemia was reduced regardless of disease severity. Additionally, intact, bioactive iFGF23 was elevated with cKL delivery in parallel with changes in genes associated with a shift in the balance of inactive cFGF23 to iFGF23, supporting the idea that cKL may alter FGF23 processing. Collectively, these findings support the concept that treatment with cKL promotes the expression of genes associated with stabilizing active iFGF23 and targeting Klotho-responsive pathways could potentially provide therapeutic benefit across disease stages in DN.

METHODS

Animal studies. Animal studies were performed according to a protocol approved by the Institutional Animal Care and Use Committee for Indiana University and the internal review board at Eli Lilly and Company and comply with the National Institutes of Health guidelines for the use of animals. Adeno-associated virus 2/8 expressing cKL (AAV-cKL) or AAV-LacZ was delivered to *db/db* uninephrectomized (*db/db*-uni) mice via retro-orbital injection at 1×10^{11} genomic copies per mouse as previously described (68). Used as "lean," normal age-matched controls, *db/dm* mice were not treated. Body weights and interim bleeds were taken at indicated times, and all mice were euthanized after 6 wk of treatment using CO_2 inhalation and then cervical dislocation.

Uninephrectomy. Uninephrectomy surgery was performed at Harlan Laboratories (Indianapolis, IN) at 4 wk of age, and mice were shipped 1 wk postsurgery. The ACR was measured on the Hitachi analyzer (Roche Diagnostics). The creatinine was measured using Roche's Creatinine Plus reagent, and the albumin was measured using Eli Lilly's modified assay. ACR was calculated as albumin/creatinine × 100 and reported as a percentage. Prior to the start of the study, all mice were rank ordered by their urine ACR from low to high. The lowest 24 were designated as the low-ACR group, whereas the highest 32 animals were used in the high-ACR group. The lowest 24 ACR values were used for groups "low ACR/LacZ" (received AAV-LacZ) and "low ACR/cKL" (received AAV-cKL), whereas the 32 animals with highest ACR were used for groups "high ACR/LacZ" and "high ACR/cKL."

Recombinant cKL and FGF23 and AAV-cKL production. As previously reported (30, 68), the cDNA encoding residues 35–983 of the extracellular domain of mouse α-KL (cKL) with a CD33 NH_2-terminal signal sequence, or β-galactosidase gene cassette (LacZ) as a vector control, was packaged into a recombinant hybrid AAV vector (RegenX Biosciences). Both AAV-cKL and AAV-LacZ localize to the liver, as previously reported (30). Recombinant cKL (mouse) and FGF23 (human) were purchased from R&D Systems.

Histology. Kidneys from the *db/dm* (lean) or *db/db*-uni mice were removed at euthanasia and fixed for at least 24 h in 10% neutral buffered formalin. Tissues were trimmed, routinely processed, embedded in paraffin and sectioned, and then stained with hematoxylin-eosin (H&E), Masson's trichrome (MTS), or periodic acid-Schiff (PAS) stains. Histopathological evaluation of these slides was conducted by an American College of Veterinary Pathologists-certified pathologist using an internally established grading system.

Serum and urine biochemistries. Whole blood was collected from tail sticks at times stated. Standard calcium, inorganic phosphorus, and BUN reagent kits were utilized for serum measurements in a Hitachi analyzer (Roche Diagnostics). Serum cKL was measured as previously described (68); serum FGF23 was tested using "Intact" FGF23 ELISA (Quidel) and "C-Term" FGF23 ELISA (Quidel). Blood glucose measurements in the lean controls and *db/db*-uni mice were performed using a Roche Aviva Accu-Chek glucometer. Urine ACR was obtained through spot urine collections over a 2–3-h period and analyzed as previously described (27).

Cell culture and in vitro functional assays. UMR-106 cells (American Type Culture Collection) were cultured in DMEM/F-12 (Invitrogen) supplemented with 10% fetal bovine serum (Hyclone), 1 mM sodium pyruvate, 25 mM L-glutamine, and 25 mM penicillin-streptomycin (Sigma-Aldrich) at 37°C and 5% CO_2. Cells were plated at 1.0×10^5 cells per well in 12-well plates and treated for 18 h with doses of cKL (30 nM) and FGF23 (115 nM) before RNA extraction.

RNA isolation and quantitative PCR. RNA from UMR-106 cells was isolated from cellular lysates using the RNeasy kit (Qiagen). RNA samples were tested by quantitative PCR with primers specific for rat *DMP1*, *FAM20C*, *GALNT3*, *FGFR1*, *FGFR2*, *FGFR3*, *FGFR4*, and internal control β-actin (*ACTB*) as previously described (16). The TaqMan One-Step RT-PCR kit (Life Technologies) was used to perform quantitative PCR, and data were collected using the 7500 Real Time PCR system and software (Life Technologies) and then analyzed using the comparative threshold cycle ($2^{-\Delta\Delta Ct}$) method (46).

Statistical analyses. Significance between groups was assessed using ANOVA analysis with a Tukey honestly significant difference post hoc test. Significance for all tests was set at $P < 0.05$, and data are presented as means ± SE.

RESULTS

cKL delivery partially corrects defective mineral metabolism in db/db-uni mice. Extensive immunohistochemistry was performed on *db/db*-uni mice to examine the similarities of this model to the clinical presentation of patients with DN. Performing uninephrectomy surgery on *db/db* mice at 4 wk of age led to marked renal pathogenesis (Fig. 1, *B*, *D*, and *F*) compared with lean controls (Fig. 1, *A*, *C*, and *E*). In this regard, H&E-stained sections of *db/db*-uni mice revealed a dilated renal pelvis (RP) with focally extensive inflammatory infiltrate (black arrows) that extended into the transitional epithelial lining (Fig. 1*B*). Similar to other studies, we found that MTS-stained sections depicted increased fibroplasia in glomeruli (increased blue matrix) with a relative paucity of open capillary loops (Fig. 1*D*; yellow arrows) compared with the normal glomeruli in lean controls (Fig. 1*C*, stars; 14, 29). Minimal interstitial fibrosis between the tubules is also highlighted in blue (Fig. 1*D*). PAS-stained sections demonstrated normal mesangial matrix and open capillary loops (Fig. 1*E*, stars). Significantly increased mesangial matrix deposition was present that frequently obliterated the normal capillary loops (Fig. 1*F*, yellow arrows) and cellularity in the glomeruli (Fig. 1*E* compared with Fig. 1*F*). Open and closed capillary loops can be a function of tissue sectioning. However, in the presence of a pathological process that involves increased mesangial matrix and other changes in the glomerular architecture along with the uniformity of closed capillary loops observed, we attributed this change to the pathological process itself and not effects of the tissue-sectioning process. Glomeruli in *db/db*-uni LacZ mice were also slightly larger than in the lean mice, potentially because of functional hypertrophy subsequent to uninephrectomy (Fig. 1*F*). These collective phenotypes are similar to those of patients with DN (19), thus providing a suitable model to explore cKL function in renal disease.

To examine the effects of cKL on DN phenotypes, the *db/db*-uni mice were treated with AAV-cKL or AAV-LacZ for 6 wk after the mice were segregated into mild-stage (low ACR) or moderate-stage (high ACR) CKD groups. For baseline references, lean control mice were used without AAV-cKL treatment. The lean

mice were significantly lower in weight than all *db/db*-uni mice, regardless of ACR or treatment (Fig. 1*G*; $P < 0.05$). Heart weight-to-body weight ratios of the *db/db*-uni mouse groups were reduced compared with lean controls because of the elevated body weights of the *db/db*-uni mice but were not different across *db/db*-uni groups (Fig. 1*H*; $P < 0.05$). Creatinine was elevated in the low-ACR/LacZ, high-ACR/LacZ, and high-ACR/cKL groups (Fig. 2*A*; $P < 0.05$), and BUN was significantly higher in high ACR/LacZ compared with lean mice (Fig. 2*B*; $P < 0.01$ vs. lean). AAV-cKL treatment was associated with partially normalized BUN in the high-ACR group (Fig. 2*B*; $P < 0.01$ vs. high ACR/LacZ). Blood glucose of lean control mice was significantly lower than that of all *db/db*-uni mice (Fig. 2*C*; $P < 0.01$). Two weeks of AAV-cKL treatment led to significantly lower blood glucose values in the high-ACR/cKL group (Fig. 2*C*; $P < 0.05$). Elevated FGF23 has been shown to be directly associated with cardiac hypertrophy (17, 26, 50). Although we observed significantly increased FGF23 with cKL delivery, we detected no changes in myocardial degeneration or fibrosis (not shown).

The *db/db*-uni mice in both the low-ACR/LacZ and high-ACR/LacZ groups were hyperphosphatemic compared with lean controls at euthanasia (Fig. 3*A*; $P < 0.01$). After AAV-cKL administration, serum phosphate was significantly reduced compared with AAV-LacZ controls in both the low- and high-ACR groups (Fig. 3*A*; $P < 0.01$). In addition, AAV-cKL treatment in high-ACR *db/db*-uni mice significantly reduced serum phosphate compared with lean mice (Fig. 3*A*; $P < 0.01$). With AAV-cKL delivery, serum Klotho levels in *db/db*-uni mice were significantly increased, in agreement with previous studies (Fig. 3*B*; $P < 0.01$; 30, 68). AAV-cKL treatment was also associated with reduced serum calcium in the low- and high-ACR groups (Fig. 3*C*; $P < 0.05$ vs. respective ACR/LacZ). The *db/db*-uni mice, regardless of ACR levels, had elevated serum alkaline phosphatase (Fig. 3*D*; $P < 0.05$ vs. lean). Treatment with AAV-cKL further elevated serum alkaline phosphatase in low- and high-ACR groups (Fig. 3*D*; $P < 0.05$ vs. respective ACR/LacZ). Thus, cKL delivery was associated with a reduction in serum phosphate, and this effect occurred under both mild and moderately severe disease conditions.

Changes in genes associated with FGF23 processing. Interestingly, cKL treatment strongly induced iFGF23 (and, predictably, cFGF23 since both circulating species are measured by the cFGF23 ELISA) in the low- and high-ACR/cKL groups at 4 and 6 wk post-AAV-cKL injection (Fig. 4, *A* and *B*; $P < 0.01$). Therefore, cKL may influence the normal cellular regulation of iFGF23 production through influencing processing of the mature hormone. To test genes potentially associated with controlling circulating iFGF23-to-cFGF23 ratios, the UMR-106 osteoblastic cell line was treated overnight with cKL either alone (30 nM) or in combination with FGF23 (115 nM). Expression of the pro-iFGF23 enzyme GALNT3 mRNA increased 2.2-fold, whereas the expression of mRNAs encoding the iFGF23-destabilizing genes DMP1 and FAM20C increased 10.5- and 5.5-fold respectively, potentially as a compensatory response following cKL+FGF23 delivery (Fig. 5*A*; $P < 0.01$). cKL treatment alone did not induce changes in GALNT3, DMP1, or FAM20C. FGFR expression was affected by cKL and FGF23 treatment, as FGFR1, FGFR2, and FGFR3, but not FGFR4, were significantly reduced after overnight treatment (Fig. 5*B*; $P < 0.05$).

In sum, we found that stable delivery of cKL to a model of DN improved hyperphosphatemia in both mild and moderate stages of kidney disease. Treatment with cKL led to a shift in proportional increases of intact, bioactive iFGF23 and cFGF23. Our findings support the concept that targeting Klotho-responsive pathways could be therapeutically beneficial across various stages of DN.

DISCUSSION

DN is one of the primary causes of end-stage renal disease and is becoming increasingly prevalent because of the increase in type 2 diabetes. To begin to understand the role of cKL and FGF23 in DN, we used a DN mouse model derived through uninephrectomy of the *db/db* diabetic mouse. We segregated *db/db*-uni mice into mild “low ACR” and moderate “high ACR” kidney disease, allowing analysis of the effects of cKL

across a CKD severity spectrum. Glomerular filtration rate was not directly assessed but could be considered in future studies. The *db/db*-uni model has been used to examine pharmacological inhibitors in the prevention of diabetic renal injury (29, 55, 71). In this regard, short-term administration of plasminogen activator inhibitor-1 (PAI-1) slowed the progression of glomerulosclerosis but had no effect on blood glucose or creatinine (29). Similarly, glomerulosclerosis was reduced by frequent and prolonged administration of an antagonist of the monocyte chemoattractant C-C chemokine ligand 2 (CCL2) but did not lower *db/db*-uni blood glucose (55). The insulin sensitizer, rosiglitazone, reduced glomerulosclerosis and lowered serum creatinine and albuminuria (71). Recently, a combination treatment of a PAI-1 neutralizing antibody and enalapril, a blood pressure-reducing agent, has shown some promise in slowing DN in *db/db*-uni mice by reducing albuminuria and markers of renal fibrosis (25). Since elevated blood phosphate is associated with more rapid CKD progression in patients (34, 64), combination therapies with the agents above and AAV-cKL could potentially lessen overall disease burden.

In our analysis, the *db/db*-uni mice were apportioned into low- and high-ACR groups to test whether AAV-cKL could improve outcomes across several CKD stages. Prior DN animal studies grouped mice by reduction in kidney function from administering low or high doses of streptozotocin (STZ; 36, 53). Higher doses of STZ resulted in increased albuminuria and worse glomerular filtration rate compared with the lower STZ dose. Interesting, AAV-cKL was associated with reducing serum phosphate regardless of kidney function status, but whether this activity was solely due to the increase in FGF23 or through direct actions of cKL on the kidney phosphate transporter activity (11, 28, 65, 69) remains to be determined. In future experiments, examination of fractional excretion of phosphate could gauge kidney tubular function and confirm mechanistically that the reduced serum phosphate occurred through increased phosphate excretion. Therefore, our results suggest that targeting cKL-mediated pathways in both mild and moderate CKD disease states would provide benefit in ameliorating defective mineral metabolism.

It is well established that patients with CKD have increased cardiovascular morbidity, particularly those in the advanced stages of renal disease (5, 20, 23). We found no definitive evidence of LVH in *db/db*-uni mice compared with lean control mice in both mild and moderate disease groups. Previous work in *db/db* mice reported a reduction in myocardial degeneration via changes in the expression patterns of cardiac remodeling genes after administration of phlorizin, a competitive inhibitor of glucose storage (8). Importantly, FGF23 has been associated with adverse patient outcomes for cardiac disease (38, 59, 66). Although cKL delivery increased FGF23, we found no increase in heart weight-to-body weight ratios, suggesting potential protective effects of cKL in the *db/db*-uni mice. Whether cKL protects heart function through inhibiting off-target FGF23 activity remains unknown. We did not detect cardiac calcifications in the *db/db*-uni model at baseline; however, when *db/db*-uni mice were fed a high-phosphate diet, renal calcification and cardiac dysfunction were reported to occur (14). We have shown AAV-cKL delivery to be capable of reducing hyperphosphatemia-induced calcification (30); thus, future work could expand cKL's utility by examining AAV-cKL administration in *db/db*-uni mice fed a high-phosphate diet.

Six weeks of cKL administration led to an increase in bioactive iFGF23 and a corresponding decrease in serum phosphate, similar to our findings in prior work (30, 68). Interestingly, cKL treatment increased iFGF23 and cFGF23, resulting in a nearly 1:1 iFGF23-to-cFGF23 ratio. This result contrasts with previous findings of FGF23 proteolytic processing during other metabolic challenges, including states of iron deficiency anemia (16). In this regard, wild-type mice responded to anemia by cleaving mature FGF23 to maintain normal blood iFGF23, leading to marked elevation in cFGF23 fragments. Additionally, patients with hyperphosphatemic familial tumoral calcinosis due to *FGF23* or *GALNT3* mutations have increased proteolysis of iFGF23, resulting in low serum concentrations of bioactive hormone. The molecular nature of the increased iFGF23-to-cFGF23 ratio in response to cKL administration remains to be determined, but this could be a potential avenue for increasing blood concentrations of iFGF23 when deficient.

Our in vitro studies support the idea that a change in FGF23 processing occurs after treatment with cKL+FGF23, as GALNT3 mRNA increased, which would favor production of iFGF23. We also found that the mRNAs from genes that are associated with FGF23 cleavage, including DMP1 and FAM20C, were increased. This result may suggest a potential compensatory response mechanism to balance iFGF23-to-cFGF23 ratios. The gene DMP1 has been previously determined to be mutated in patients with autosomal recessive hypophosphatemic rickets, resulting in marked upregulation of iFGF23 (15). In agreement with this phenotype, FGF23 mRNA and iFGF23 are significantly increased in osteoblast/osteocyte-specific DMP1-conditional and global DMP1 knockout mice (18). Importantly, the genetic loss of DMP1 and the overexpression of cKL are similar in that they result in overriding the typically suppressive effects of hypophosphatemia on suppressing FGF23 production (1). Certainly, the exact mechanisms guiding iFGF23-to-cFGF23 ratios due to dynamic changes in mRNA expression, protein production, and activity of intracellular protein-processing systems in osteoblasts/osteocytes remain to be fully resolved.

In sum, our results demonstrate that providing cKL in DN can reduce serum phosphate during mild and moderate disease states, as well as potentially ameliorate other biochemical outcomes, supporting the concept of targeting cKL-mediated pathways for control of mineral metabolism.

GRANTS

We acknowledge support from NIH Grants R01-DK-063934 and R01-DK-95784 (K. E. White), T32-HL-007910 (J. M. Hum), and F32-AR-065389 (E. L. Clinkenbeard); the Indiana Genomics Initiative of Indiana University, supported in part by the Lilly Endowment, Inc. (K. E. White); a Showalter Scholar award supported through the Ralph W. and Grace M. Showalter Research Trust Fund (K. E. White); and Faculty Research Development grants from Marian University's College of Osteopathic Medicine (J. M. Hum).

DISCLOSURES

L. M. O'Bryan, R. C. Smith, M. S. Cramer, M. Bhaskaran, R. L. Johnson, and J. M. Wilson were all employees of Eli Lilly & Co. at the time of the study. A. K. Tatiparthi is an employee of Covance, Inc. K. E. White received royalties from Kyowa Hakko Kirin Co., Ltd. for licensing of the FGF23 gene and the anti-FGF23 monoclonal antibody clinical trials, and has had research funding from Eli Lilly. None of the other authors has any conflicts of interest, financial or otherwise, to disclose.

AUTHOR CONTRIBUTIONS

R.C.S., L.M.O., M.S.C., J.M.H., and K.E.W. conceived and designed research; L.M.O., A.K.T., M.S.C., M.B., R.L.J., J.M.W., and R.C.S. performed experiments; J.M.H., L.M.O., E.L.C., P.N., R.C.S., and K.E.W. analyzed data; J.M.H., L.M.O., R.C.S., and K.E.W. interpreted results of experiments; J.M.H., L.M.O., R.C.S., and K.E.W. prepared figures; J.M.H., L.M.O., R.C.S., and K.E.W. drafted manuscript; J.M.H., L.M.O., R.C.S., and K.E.W. edited and revised manuscript; J.M.H., L.M.O., R.C.S., and K.E.W. approved final version of manuscript.

REFERENCES

1. Antoniucci DM, Yamashita T, Portale AA. Dietary phosphorus regulates serum fibroblast growth factor-23 concentrations in healthy men. J Clin Endocrinol Metab 91: 3144–3149, 2006. doi:10.1210/jc.2006-0021. [PubMed: 16735491] [CrossRef: 10.1210/jc.2006-0021]

2. Asai O, Nakatani K, Tanaka T, Sakan H, Imura A, Yoshimoto S, Samejima K, Yamaguchi Y, Matsui M, Akai Y, Konishi N, Iwano M, Nabeshima Y, Saito Y. Decreased renal α-Klotho expression in early diabetic nephropathy in humans and mice and its possible role in urinary calcium excretion. Kidney Int 81:

539–547, 2012. doi:10.1038/ki.2011.423. [PubMed: 22217880] [CrossRef: 10.1038/ki.2011.423]

3. Beck L, Soumounou Y, Martel J, Krishnamurthy G, Gauthier C, Goodyer CG, Tenenhouse HS. Pex/PEX tissue distribution and evidence for a deletion in the 3′ region of the Pex gene in X-linked hypophosphatemic mice. J Clin Invest 99: 1200–1209, 1997. doi:10.1172/JCI119276. [PMCID: PMC507933] [PubMed: 9077527] [CrossRef: 10.1172/JCI119276]

4. Bergwitz C, Banerjee S, Abu-Zahra H, Kaji H, Miyauchi A, Sugimoto T, Jüppner H. Defective O-glycosylation due to a novel homozygous S129P mutation is associated with lack of fibroblast growth factor 23 secretion and tumoral calcinosis. J Clin Endocrinol Metab 94: 4267–4274, 2009. doi:10.1210/jc.2009-0961. [PMCID: PMC2775647] [PubMed: 19837926] [CrossRef: 10.1210/jc.2009-0961]

5. Block GA, Klassen PS, Lazarus JM, Ofsthun N, Lowrie EG, Chertow GM. Mineral metabolism, mortality, and morbidity in maintenance hemodialysis. J Am Soc Nephrol 15: 2208–2218, 2004. doi:10.1097/01.ASN.0000133041.27682.A2. [PubMed: 15284307] [CrossRef: 10.1097/01.ASN.0000133041.27682.A2]

6. Bower G, Brown DM, Steffes MW, Vernier RL, Mauer SM. Studies of the glomerular mesangium and the juxtaglomerular apparatus in the genetically diabetic mouse. Lab Invest 43: 333–341, 1980. [PubMed: 7003252]

7. Braithwaite V, Prentice AM, Doherty C, Prentice A. FGF23 is correlated with iron status but not with inflammation and decreases after iron supplementation: a supplementation study. Int J Pediatr Endocrinol 2012: 27, 2012. doi:10.1186/1687-9856-2012-27. [PMCID: PMC3523041] [PubMed: 23098062] [CrossRef: 10.1186/1687-9856-2012-27]

8. Cai Q, Li B, Yu F, Lu W, Zhang Z, Yin M, Gao H. Investigation of the protective effects of phlorizin on diabetic cardiomyopathy in *db/db* mice by quantitative proteomics. J Diabetes Res 2013: 263845, 2013. doi:10.1155/2013/263845. [PMCID: PMC3647560] [PubMed: 23671862] [CrossRef: 10.1155/2013/263845]

9. Chen H, Charlat O, Tartaglia LA, Woolf EA, Weng X, Ellis SJ, Lakey ND, Culpepper J, Moore KJ, Breitbart RE, Duyk GM, Tepper RI, Morgenstern JP. Evidence that the diabetes gene encodes the leptin receptor: identification of a mutation in the leptin receptor gene in *db/db* mice. Cell 84: 491–495, 1996. doi:10.1016/S0092-8674(00)81294-5. [PubMed: 8608603] [CrossRef: 10.1016/S0092-8674(00)81294-5]

10. Clinkenbeard EL, Farrow EG, Summers LJ, Cass TA, Roberts JL, Bayt CA, Lahm T, Albrecht M, Allen MR, Peacock M, White KE. Neonatal iron deficiency causes abnormal phosphate metabolism by elevating FGF23 in normal and ADHR mice. J Bone Miner Res 29: 361–369, 2014. doi:10.1002/jbmr.2049. [PMCID: PMC5240191] [PubMed: 23873717] [CrossRef: 10.1002/jbmr.2049]

11. Dërmaku-Sopjani M, Sopjani M, Saxena A, Shojaiefard M, Bogatikov E, Alesutan I, Eichenmüller M, Lang F. Downregulation of NaPi-IIa and NaPi-IIb Na-coupled phosphate transporters by coexpression of Klotho. Cell Physiol Biochem 28: 251–258, 2011. doi:10.1159/000331737. [PubMed: 21865732] [CrossRef: 10.1159/000331737]

12. Econs MJ, Francis F. Positional cloning of the PEX gene: new insights into the pathophysiology of X-linked hypophosphatemic rickets. Am J Physiol Renal Physiol 273: F489–F498, 1997. doi:10.1152/ajprenal.1997.273.4.F489. [PubMed: 9362326] [CrossRef: 10.1152/ajprenal.1997.273.4.F489]

13. Econs MJ, McEnery PT. Autosomal dominant hypophosphatemic rickets/osteomalacia: clinical characterization of a novel renal phosphate-wasting disorder. J Clin Endocrinol Metab 82: 674–681, 1997. doi:10.1210/jcem.82.2.3765. [PubMed: 9024275] [CrossRef: 10.1210/jcem.82.2.3765]

14. Eller P, Eller K, Kirsch AH, Patsch JJ, Wolf AM, Tagwerker A, Stanzl U, Kaindl R, Kahlenberg V, Mayer G, Patsch JR, Rosenkranz AR. A murine model of phosphate nephropathy. Am J Pathol 178: 1999–2006, 2011. doi:10.1016/j.ajpath.2011.01.024. [PMCID: PMC3081192] [PubMed: 21514417] [CrossRef: 10.1016/j.ajpath.2011.01.024]

15. Farrow EG, Davis SI, Ward LM, Summers LJ, Bubbear JS, Keen R, Stamp TC, Baker LR, Bonewald LF, White KE. Molecular analysis of DMP1 mutants causing autosomal recessive hypophosphatemic rickets. Bone 44: 287–294, 2009. doi:10.1016/j.bone.2008.10.040. [PMCID: PMC2669955] [PubMed: 19007919] [CrossRef: 10.1016/j.bone.2008.10.040]

16. Farrow EG, Yu X, Summers LJ, Davis SI, Fleet JC, Allen MR, Robling AG, Stayrook KR, Jideonwo V, Magers MJ, Garringer HJ, Vidal R, Chan RJ, Goodwin CB, Hui SL, Peacock M, White KE. Iron deficiency drives an autosomal dominant hypophosphatemic rickets (ADHR) phenotype in fibroblast growth factor-23 (Fgf23) knock-in mice. Proc Natl Acad Sci USA 108: E1146–E1155, 2011. doi:10.1073/pnas.1110905108. [PMCID: PMC3219119] [PubMed: 22006328] [CrossRef: 10.1073/pnas.1110905108]

17. Faul C, Amaral AP, Oskouei B, Hu MC, Sloan A, Isakova T, Gutiérrez OM, Aguillon-Prada R, Lincoln J, Hare JM, Mundel P, Morales A, Scialla J, Fischer M, Soliman EZ, Chen J, Go AS, Rosas SE, Nessel L, Townsend RR, Feldman HI, St John Sutton M, Ojo A, Gadegbeku C, Di Marco GS, Reuter S, Kentrup D, Tiemann K, Brand M, Hill JA, Moe OW, Kuro-O M, Kusek JW, Keane MG, Wolf M. FGF23 induces left ventricular hypertrophy. J Clin Invest 121: 4393–4408, 2011. doi:10.1172/JCI46122. [PMCID: PMC3204831] [PubMed: 21985788] [CrossRef: 10.1172/JCI46122]

18. Feng JQ, Ward LM, Liu S, Lu Y, Xie Y, Yuan B, Yu X, Rauch F, Davis SI, Zhang S, Rios H, Drezner MK, Quarles LD, Bonewald LF, White KE. Loss of DMP1 causes rickets and osteomalacia and identifies a role for osteocytes in mineral metabolism. Nat Genet 38: 1310–1315, 2006. doi:10.1038/ng1905. [PMCID: PMC1839871] [PubMed: 17033621] [CrossRef: 10.1038/ng1905]

19. Fioretto P, Mauer M. Histopathology of diabetic nephropathy. Semin Nephrol 27: 195–207, 2007. doi:10.1016/j.semnephrol.2007.01.012. [PMCID: PMC2746982] [PubMed: 17418688] [CrossRef: 10.1016/j.semnephrol.2007.01.012]

20. Foley RN, Murray AM, Li S, Herzog CA, McBean AM, Eggers PW, Collins AJ. Chronic kidney disease and the risk for cardiovascular disease, renal replacement, and death in the United States Medicare population, 1998 to 1999. J Am Soc Nephrol 16: 489–495, 2005. doi:10.1681/ASN.2004030203. [PubMed: 15590763] [CrossRef: 10.1681/ASN.2004030203]

21. Gaikwad AB, Sayyed SG, Lichtnekert J, Tikoo K, Anders HJ. Renal failure increases cardiac histone h3 acetylation, dimethylation, and phosphorylation and the induction of cardiomyopathy-related genes in type 2 diabetes. Am J Pathol 176: 1079–1083, 2010. doi:10.2353/ajpath.2010.090528. [PMCID: PMC2832129] [PubMed: 20075197] [CrossRef: 10.2353/ajpath.2010.090528]

22. Ghosh B, Brojen T, Banerjee S, Singh N, Singh S, Sharma OP, Prakash J. The high prevalence of chronic kidney disease-mineral bone disorders: a hospital-based cross-sectional study. Indian J Nephrol 22: 285–291, 2012. doi:10.4103/0971-4065.101249. [PMCID: PMC3495351] [PubMed: 23162273] [CrossRef: 10.4103/0971-4065.101249]

23. Go AS, Chertow GM, Fan D, McCulloch CE, Hsu CY. Chronic kidney disease and the risks of death, cardiovascular events, and hospitalization. N Engl J Med 351: 1296–1305, 2004. doi:10.1056/NEJMoa041031. [PubMed: 15385656] [CrossRef: 10.1056/NEJMoa041031]

24. Goetz R, Nakada Y, Hu MC, Kurosu H, Wang L, Nakatani T, Shi M, Eliseenkova AV, Razzaque MS, Moe OW, Kuro-o M, Mohammadi M. Isolated C-terminal tail of FGF23 alleviates hypophosphatemia by

inhibiting FGF23-FGFR-Klotho complex formation. Proc Natl Acad Sci USA 107: 407–412, 2010. doi:10.1073/pnas.0902006107. [PMCID: PMC2806769] [PubMed: 19966287] [CrossRef: 10.1073/pnas.0902006107]

25. Gu C, Zhang J, Noble NA, Peng XR, Huang Y. An additive effect of anti-PAI-1 antibody to ACE inhibitor on slowing the progression of diabetic kidney disease. Am J Physiol Renal Physiol 311: F852–F863, 2016. doi:10.1152/ajprenal.00564.2015. [PMCID: PMC5130463] [PubMed: 27511457] [CrossRef: 10.1152/ajprenal.00564.2015]

26. Gutiérrez OM, Mannstadt M, Isakova T, Rauh-Hain JA, Tamez H, Shah A, Smith K, Lee H, Thadhani R, Jüppner H, Wolf M. Fibroblast growth factor 23 and mortality among patients undergoing hemodialysis. N Engl J Med 359: 584–592, 2008. doi:10.1056/NEJMoa0706130. [PMCID: PMC2890264] [PubMed: 18687639] [CrossRef: 10.1056/NEJMoa0706130]

27. Harlan SM, Ostroski RA, Coskun T, Yantis LD, Breyer MD, Heuer JG. Viral transduction of renin rapidly establishes persistent hypertension in diverse murine strains. Am J Physiol Regul Integr Comp Physiol 309: R467–R474, 2015. doi:10.1152/ajpregu.00106.2015. [PubMed: 26108870] [CrossRef: 10.1152/ajpregu.00106.2015]

28. Hu MC, Shi M, Zhang J, Pastor J, Nakatani T, Lanske B, Razzaque MS, Rosenblatt KP, Baum MG, Kuro-o M, Moe OW. Klotho: a novel phosphaturic substance acting as an autocrine enzyme in the renal proximal tubule. FASEB J 24: 3438–3450, 2010. doi:10.1096/fj.10-154765. [PMCID: PMC2923354] [PubMed: 20466874] [CrossRef: 10.1096/fj.10-154765]

29. Huang Y, Border WA, Yu L, Zhang J, Lawrence DA, Noble NA. A PAI-1 mutant, PAI-1R, slows progression of diabetic nephropathy. J Am Soc Nephrol 19: 329–338, 2008. doi:10.1681/ASN.2007040510. [PMCID: PMC2396741] [PubMed: 18216319] [CrossRef: 10.1681/ASN.2007040510]

30. Hum JM, O'Bryan LM, Tatiparthi AK, Cass TA, Clinkenbeard EL, Cramer MS, Bhaskaran M, Johnson RL, Wilson JM, Smith RC, White KE. Chronic hyperphosphatemia and vascular calcification are reduced by stable delivery of soluble Klotho. J Am Soc Nephrol 28: 1162–1174, 2017. doi:10.1681/ASN.2015111266. [PMCID: PMC5373441] [PubMed: 27837149] [CrossRef: 10.1681/ASN.2015111266]

31. Imanishi Y, Inaba M, Nakatsuka K, Nagasue K, Okuno S, Yoshihara A, Miura M, Miyauchi A, Kobayashi K, Miki T, Shoji T, Ishimura E, Nishizawa Y. FGF-23 in patients with end-stage renal disease on hemodialysis. Kidney Int 65: 1943–1946, 2004. doi:10.1111/j.1523-1755.2004.00604.x. [PubMed: 15086938] [CrossRef: 10.1111/j.1523-1755.2004.00604.x]

32. Imel EA, Peacock M, Gray AK, Padgett LR, Hui SL, Econs MJ. Iron modifies plasma FGF23 differently in autosomal dominant hypophosphatemic rickets and healthy humans. J Clin Endocrinol Metab 96: 3541–3549, 2011. doi:10.1210/jc.2011-1239. [PMCID: PMC3205884] [PubMed: 21880793] [CrossRef: 10.1210/jc.2011-1239]

33. Ishikawa HO, Xu A, Ogura E, Manning G, Irvine KD. The Raine syndrome protein FAM20C is a Golgi kinase that phosphorylates bio-mineralization proteins. PLoS One 7: e42988, 2012. doi:10.1371/journal.pone.0042988. [PMCID: PMC3416761] [PubMed: 22900076] [CrossRef: 10.1371/journal.pone.0042988]

34. Ix JH, Katz R, Kestenbaum BR, de Boer IH, Chonchol M, Mukamal KJ, Rifkin D, Siscovick DS, Sarnak MJ, Shlipak MG. Fibroblast growth factor-23 and death, heart failure, and cardiovascular events in community-living individuals: CHS (Cardiovascular Health Study). J Am Coll Cardiol 60: 200–207, 2012. doi:10.1016/j.jacc.2012.03.040. [PMCID: PMC3396791] [PubMed: 22703926] [CrossRef:

10.1016/j.jacc.2012.03.040]

35. Jonsson KB, Zahradnik R, Larsson T, White KE, Sugimoto T, Imanishi Y, Yamamoto T, Hampson G, Koshiyama H, Ljunggren O, Oba K, Yang IM, Miyauchi A, Econs MJ, Lavigne J, Jüppner H. Fibroblast growth factor 23 in oncogenic osteomalacia and X-linked hypophosphatemia. N Engl J Med 348: 1656–1663, 2003. doi:10.1056/NEJMoa020881. [PubMed: 12711740] [CrossRef: 10.1056/NEJMoa020881]

36. Kanetsuna Y, Takahashi K, Nagata M, Gannon MA, Breyer MD, Harris RC, Takahashi T. Deficiency of endothelial nitric-oxide synthase confers susceptibility to diabetic nephropathy in nephropathy-resistant inbred mice. Am J Pathol 170: 1473–1484, 2007. doi:10.2353/ajpath.2007.060481. [PMCID: PMC1854944] [PubMed: 17456755] [CrossRef: 10.2353/ajpath.2007.060481]

37. Kato K, Jeanneau C, Tarp MA, Benet-Pagès A, Lorenz-Depiereux B, Bennett EP, Mandel U, Strom TM, Clausen H. Polypeptide GalNAc-transferase T3 and familial tumoral calcinosis. Secretion of fibroblast growth factor 23 requires O-glycosylation. J Biol Chem 281: 18370–18377, 2006. doi:10.1074/jbc.M602469200. [PubMed: 16638743] [CrossRef: 10.1074/jbc.M602469200]

38. Kendrick J, Cheung AK, Kaufman JS, Greene T, Roberts WL, Smits G, Chonchol M; HOST Investigators . FGF-23 associates with death, cardiovascular events, and initiation of chronic dialysis. J Am Soc Nephrol 22: 1913–1922, 2011. doi:10.1681/ASN.2010121224. [PMCID: PMC3187186] [PubMed: 21903574] [CrossRef: 10.1681/ASN.2010121224]

39. Koh N, Fujimori T, Nishiguchi S, Tamori A, Shiomi S, Nakatani T, Sugimura K, Kishimoto T, Kinoshita S, Kuroki T, Nabeshima Y. Severely reduced production of klotho in human chronic renal failure kidney. Biochem Biophys Res Commun 280: 1015–1020, 2001. doi:10.1006/bbrc.2000.4226. [PubMed: 11162628] [CrossRef: 10.1006/bbrc.2000.4226]

40. Kuro-o M, Matsumura Y, Aizawa H, Kawaguchi H, Suga T, Utsugi T, Ohyama Y, Kurabayashi M, Kaname T, Kume E, Iwasaki H, Iida A, Shiraki-Iida T, Nishikawa S, Nagai R, Nabeshima YI. Mutation of the mouse klotho gene leads to a syndrome resembling ageing. Nature 390: 45–51, 1997. doi:10.1038/36285. [PubMed: 9363890] [CrossRef: 10.1038/36285]

41. Kurosu H, Ogawa Y, Miyoshi M, Yamamoto M, Nandi A, Rosenblatt KP, Baum MG, Schiavi S, Hu MC, Moe OW, Kuro-o M. Regulation of fibroblast growth factor-23 signaling by klotho. J Biol Chem 281: 6120–6123, 2006. doi:10.1074/jbc.C500457200. [PMCID: PMC2637204] [PubMed: 16436388] [CrossRef: 10.1074/jbc.C500457200]

42. Larsson T, Nisbeth U, Ljunggren O, Jüppner H, Jonsson KB. Circulating concentration of FGF-23 increases as renal function declines in patients with chronic kidney disease, but does not change in response to variation in phosphate intake in healthy volunteers. Kidney Int 64: 2272–2279, 2003. doi:10.1046/j.1523-1755.2003.00328.x. [PubMed: 14633152] [CrossRef: 10.1046/j.1523-1755.2003.00328.x]

43. Lee GH, Proenca R, Montez JM, Carroll KM, Darvishzadeh JG, Lee JI, Friedman JM. Abnormal splicing of the leptin receptor in diabetic mice. Nature 379: 632–635, 1996. doi:10.1038/379632a0. [PubMed: 8628397] [CrossRef: 10.1038/379632a0]

44. Li H, Martin A, David V, Quarles LD. Compound deletion of Fgfr3 and Fgfr4 partially rescues the Hyp mouse phenotype. Am J Physiol Endocrinol Metab 300: E508–E517, 2011. doi:10.1152/ajpendo.00499.2010. [PMCID: PMC3064005] [PubMed: 21139072] [CrossRef: 10.1152/ajpendo.00499.2010]

45. Liu S, Tang W, Zhou J, Stubbs JR, Luo Q, Pi M, Quarles LD. Fibroblast growth factor 23 is a counter-

regulatory phosphaturic hormone for vitamin D. J Am Soc Nephrol 17: 1305–1315, 2006. doi:10.1681/ASN.2005111185. [PubMed: 16597685] [CrossRef: 10.1681/ASN.2005111185]

46. Livak KJ, Schmittgen TD. Analysis of relative gene expression data using real-time quantitative PCR and the $2^{-\Delta\Delta CT}$ method. Methods 25: 402–408, 2001. doi:10.1006/meth.2001.1262. [PubMed: 11846609] [CrossRef: 10.1006/meth.2001.1262]

47. Lorenz-Depiereux B, Bastepe M, Benet-Pagès A, Amyere M, Wagenstaller J, Müller-Barth U, Badenhoop K, Kaiser SM, Rittmaster RS, Shlossberg AH, Olivares JL, Loris C, Ramos FJ, Glorieux F, Vikkula M, Jüppner H, Strom TM. DMP1 mutations in autosomal recessive hypophosphatemia implicate a bone matrix protein in the regulation of phosphate homeostasis. Nat Genet 38: 1248–1250, 2006. doi:10.1038/ng1868. [PMCID: PMC5942547] [PubMed: 17033625] [CrossRef: 10.1038/ng1868]

48. Massry S. K/DOQI guidelines released on bone metabolism and disease in CKD. Nephrol News Issues 17: 38–41, 2003. [PubMed: 14640009]

49. Matsumura Y, Aizawa H, Shiraki-Iida T, Nagai R, Kuro-o M, Nabeshima Y. Identification of the human klotho gene and its two transcripts encoding membrane and secreted klotho protein. Biochem Biophys Res Commun 242: 626–630, 1998. doi:10.1006/bbrc.1997.8019. [PubMed: 9464267] [CrossRef: 10.1006/bbrc.1997.8019]

50. Mirza MA, Larsson A, Melhus H, Lind L, Larsson TE. Serum intact FGF23 associate with left ventricular mass, hypertrophy and geometry in an elderly population. Atherosclerosis 207: 546–551, 2009. doi:10.1016/j.atherosclerosis.2009.05.013. [PubMed: 19524924] [CrossRef: 10.1016/j.atherosclerosis.2009.05.013]

51. Moe S, Drüeke T, Cunningham J, Goodman W, Martin K, Olgaard K, Ott S, Sprague S, Lameire N, Eknoyan G; Kidney Disease: Improving Global Outcomes (KDIGO) . Definition, evaluation, and classification of renal osteodystrophy: a position statement from Kidney Disease: Improving Global Outcomes (KDIGO). Kidney Int 69: 1945–1953, 2006. doi:10.1038/sj.ki.5000414. [PubMed: 16641930] [CrossRef: 10.1038/sj.ki.5000414]

52. Moe SM, Radcliffe JS, White KE, Gattone VH II, Seifert MF, Chen X, Aldridge B, Chen NX. The pathophysiology of early-stage chronic kidney disease-mineral bone disorder (CKD-MBD) and response to phosphate binders in the rat. J Bone Miner Res 26: 2672–2681, 2011. doi:10.1002/jbmr.485. [PubMed: 21826734] [CrossRef: 10.1002/jbmr.485]

53. Nakagawa T, Sato W, Glushakova O, Heinig M, Clarke T, Campbell-Thompson M, Yuzawa Y, Atkinson MA, Johnson RJ, Croker B. Diabetic endothelial nitric oxide synthase knockout mice develop advanced diabetic nephropathy. J Am Soc Nephrol 18: 539–550, 2007. doi:10.1681/ASN.2006050459. [PubMed: 17202420] [CrossRef: 10.1681/ASN.2006050459]

54. National Kidney Foundation K/DOQI clinical practice guidelines for bone metabolism and disease in chronic kidney disease. Am J Kidney Dis 42, Suppl 3: S1–S201, 2003. doi:10.1016/S0272-6386(03)00905-3. [PubMed: 14520607] [CrossRef: 10.1016/S0272-6386(03)00905-3]

55. Ninichuk V, Clauss S, Kulkarni O, Schmid H, Segerer S, Radomska E, Eulberg D, Buchner K, Selve N, Klussmann S, Anders HJ. Late onset of Ccl2 blockade with the Spiegelmer mNOX-E36-3′PEG prevents glomerulosclerosis and improves glomerular filtration rate in *db/db* mice. Am J Pathol 172: 628–637, 2008. doi:10.2353/ajpath.2008.070601. [PMCID: PMC2258250] [PubMed: 18258851] [CrossRef: 10.2353/ajpath.2008.070601]

56. Ninichuk V, Khandoga AG, Segerer S, Loetscher P, Schlapbach A, Revesz L, Feifel R, Khandoga A, Krombach F, Nelson PJ, Schlöndorff D, Anders HJ. The role of interstitial macrophages in nephropathy of

type 2 diabetic *db/db* mice. Am J Pathol 170: 1267–1276, 2007. doi:10.2353/ajpath.2007.060937. [PMCID: PMC1829460] [PubMed: 17392166] [CrossRef: 10.2353/ajpath.2007.060937]

57. Ninichuk V, Kulkarni O, Clauss S, Anders H. Tubular atrophy, interstitial fibrosis, and inflammation in type 2 diabetic *db/db* mice. An accelerated model of advanced diabetic nephropathy. Eur J Med Res 12: 351–355, 2007. [PubMed: 17933712]

58. Olauson H, Lindberg K, Amin R, Jia T, Wernerson A, Andersson G, Larsson TE. Targeted deletion of Klotho in kidney distal tubule disrupts mineral metabolism. J Am Soc Nephrol 23: 1641–1651, 2012. doi:10.1681/ASN.2012010048. [PMCID: PMC3458458] [PubMed: 22878961] [CrossRef: 10.1681/ASN.2012010048]

59. Parker BD, Schurgers LJ, Brandenburg VM, Christenson RH, Vermeer C, Ketteler M, Shlipak MG, Whooley MA, Ix JH. The associations of fibroblast growth factor 23 and uncarboxylated matrix Gla protein with mortality in coronary artery disease: the Heart and Soul Study. Ann Intern Med 152: 640–648, 2010. doi:10.7326/0003-4819-152-10-201005180-00004. [PMCID: PMC3079370] [PubMed: 20479029] [CrossRef: 10.7326/0003-4819-152-10-201005180-00004]

60. Plantinga LC, Crews DC, Coresh J, Miller ER III, Saran R, Yee J, Hedgeman E, Pavkov M, Eberhardt MS, Williams DE, Powe NR; CDC CKD Surveillance Team . Prevalence of chronic kidney disease in US adults with undiagnosed diabetes or prediabetes. Clin J Am Soc Nephrol 5: 673–682, 2010. doi:10.2215/CJN.07891109. [PMCID: PMC2849697] [PubMed: 20338960] [CrossRef: 10.2215/CJN.07891109]

61. Prats M, Font R, García C, Cabré C, Jariod M, Vea AM. Effect of ferric carboxymaltose on serum phosphate and C-terminal FGF23 levels in non-dialysis chronic kidney disease patients: post-hoc analysis of a prospective study. BMC Nephrol 14: 167, 2013. doi:10.1186/1471-2369-14-167. [PMCID: PMC3751040] [PubMed: 23902731] [CrossRef: 10.1186/1471-2369-14-167]

62. Rafaelsen SH, Raeder H, Fagerheim AK, Knappskog P, Carpenter TO, Johansson S, Bjerknes R. Exome sequencing reveals FAM20c mutations associated with fibroblast growth factor 23-related hypophosphatemia, dental anomalies, and ectopic calcification. J Bone Miner Res 28: 1378–1385, 2013. doi:10.1002/jbmr.1850. [PubMed: 23325605] [CrossRef: 10.1002/jbmr.1850]

63. Schouten BJ, Hunt PJ, Livesey JH, Frampton CM, Soule SG. FGF23 elevation and hypophosphatemia after intravenous iron polymaltose: a prospective study. J Clin Endocrinol Metab 94: 2332–2337, 2009. doi:10.1210/jc.2008-2396. [PubMed: 19366850] [CrossRef: 10.1210/jc.2008-2396]

64. Scialla JJ, Xie H, Rahman M, Anderson AH, Isakova T, Ojo A, Zhang X, Nessel L, Hamano T, Grunwald JE, Raj DS, Yang W, He J, Lash JP, Go AS, Kusek JW, Feldman H, Wolf M; Chronic Renal Insufficiency Cohort (CRIC) Study Investigators . Fibroblast growth factor-23 and cardiovascular events in CKD. J Am Soc Nephrol 25: 349–360, 2014. doi:10.1681/ASN.2013050465. [PMCID: PMC3904568] [PubMed: 24158986] [CrossRef: 10.1681/ASN.2013050465]

65. Segawa H, Yamanaka S, Ohno Y, Onitsuka A, Shiozawa K, Aranami F, Furutani J, Tomoe Y, Ito M, Kuwahata M, Imura A, Nabeshima Y, Miyamoto K. Correlation between hyperphosphatemia and type II Na-Pi cotransporter activity in klotho mice. Am J Physiol Renal Physiol 292: F769–F779, 2007. doi:10.1152/ajprenal.00248.2006. [PubMed: 16985213] [CrossRef: 10.1152/ajprenal.00248.2006]

66. Seiler S, Reichart B, Roth D, Seibert E, Fliser D, Heine GH. FGF-23 and future cardiovascular events in patients with chronic kidney disease before initiation of dialysis treatment. Nephrol Dial Transplant 25: 3983–3989, 2010. doi:10.1093/ndt/gfq309. [PubMed: 20525642] [CrossRef: 10.1093/ndt/gfq309]

67. Sharma K, McCue P, Dunn SR. Diabetic kidney disease in the *db/db* mouse. Am J Physiol Renal

Physiol 284: F1138–F1144, 2003. doi:10.1152/ajprenal.00315.2002. [PubMed: 12736165] [CrossRef: 10.1152/ajprenal.00315.2002]

68. Smith RC, O'Bryan LM, Farrow EG, Summers LJ, Clinkenbeard EL, Roberts JL, Cass TA, Saha J, Broderick C, Ma YL, Zeng QQ, Kharitonenkov A, Wilson JM, Guo Q, Sun H, Allen MR, Burr DB, Breyer MD, White KE. Circulating αKlotho influences phosphate handling by controlling FGF23 production. J Clin Invest 122: 4710–4715, 2012. doi:10.1172/JCI64986. [PMCID: PMC3533557] [PubMed: 23187128] [CrossRef: 10.1172/JCI64986]

69. Sopjani M, Alesutan I, Dërmaku-Sopjani M, Gu S, Zelenak C, Munoz C, Velic A, Föller M, Rosenblatt KP, Kuro-o M, Lang F. Regulation of the Na^+/K^+ ATPase by Klotho. FEBS Lett 585: 1759–1764, 2011. doi:10.1016/j.febslet.2011.05.021. [PubMed: 21605558] [CrossRef: 10.1016/j.febslet.2011.05.021]

70. Tagliabracci VS, Engel JL, Wiley SE, Xiao J, Gonzalez DJ, Nidumanda Appaiah H, Koller A, Nizet V, White KE, Dixon JE. Dynamic regulation of FGF23 by Fam20C phosphorylation, GalNAc-T3 glycosylation, and furin proteolysis. Proc Natl Acad Sci USA 111: 5520–5525, 2014. doi:10.1073/pnas.1402218111. [PMCID: PMC3992636] [PubMed: 24706917] [CrossRef: 10.1073/pnas.1402218111]

71. Tang SC, Leung JC, Chan LY, Cheng AS, Lan HY, Lai KN. Renoprotection by rosiglitazone in accelerated type 2 diabetic nephropathy: role of STAT1 inhibition and nephrin restoration. Am J Nephrol 32: 145–155, 2010. doi:10.1159/000316056. [PubMed: 20606418] [CrossRef: 10.1159/000316056]

72. Urakawa I, Yamazaki Y, Shimada T, Iijima K, Hasegawa H, Okawa K, Fujita T, Fukumoto S, Yamashita T. Klotho converts canonical FGF receptor into a specific receptor for FGF23. Nature 444: 770–774, 2006. doi:10.1038/nature05315. [PubMed: 17086194] [CrossRef: 10.1038/nature05315]

73. White KE, Carn G, Lorenz-Depiereux B, Benet-Pages A, Strom TM, Econs MJ. Autosomal-dominant hypophosphatemic rickets (ADHR) mutations stabilize FGF-23. Kidney Int 60: 2079–2086, 2001. doi:10.1046/j.1523-1755.2001.00064.x. [PubMed: 11737582] [CrossRef: 10.1046/j.1523-1755.2001.00064.x]

74. Yamazaki Y, Okazaki R, Shibata M, Hasegawa Y, Satoh K, Tajima T, Takeuchi Y, Fujita T, Nakahara K, Yamashita T, Fukumoto S. Increased circulatory level of biologically active full-length FGF-23 in patients with hypophosphatemic rickets/osteomalacia. J Clin Endocrinol Metab 87: 4957–4960, 2002. doi:10.1210/jc.2002-021105. [PubMed: 12414858] [CrossRef: 10.1210/jc.2002-021105]

75. Yuan B, Takaiwa M, Clemens TL, Feng JQ, Kumar R, Rowe PS, Xie Y, Drezner MK. Aberrant Phex function in osteoblasts and osteocytes alone underlies murine X-linked hypophosphatemia. J Clin Invest 118: 722–734, 2008. doi:10.1172/JCI32702. [PMCID: PMC2157563] [PubMed: 18172553] [CrossRef: 10.1172/JCI32702]

Figures and Tables

Fig. 1.

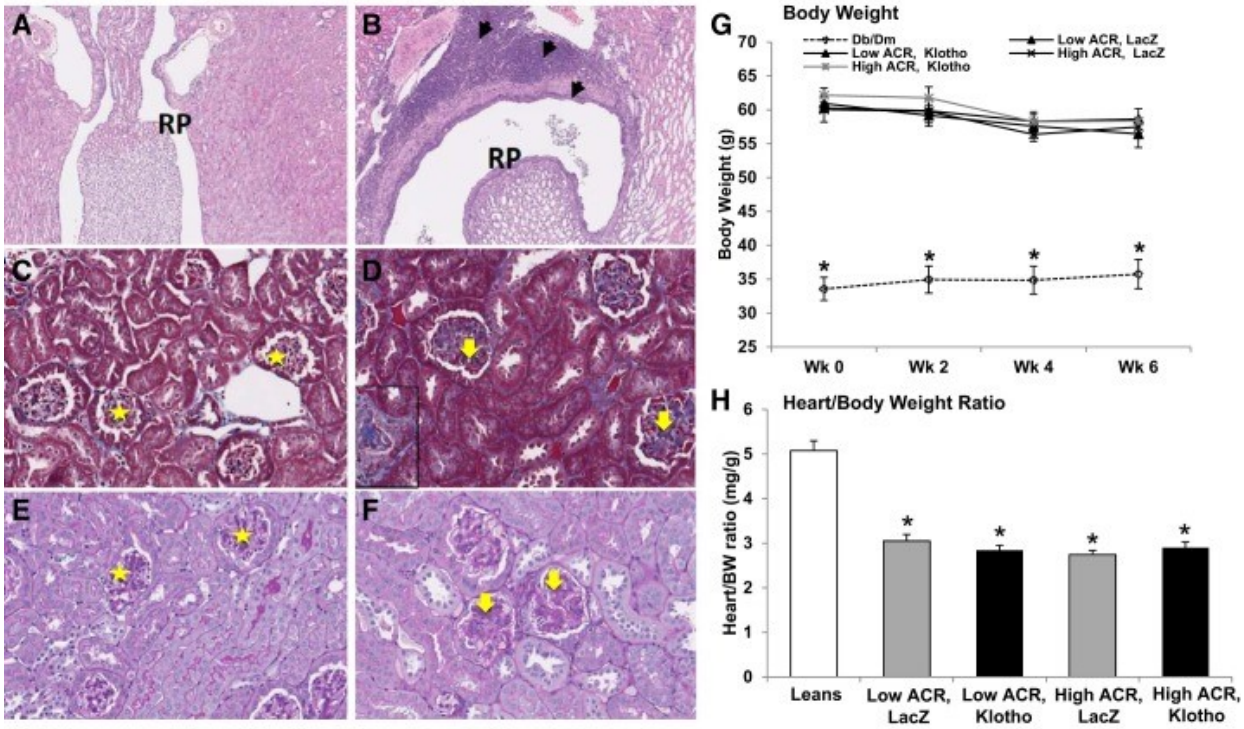

Various stages of diabetic nephropathy are exhibited by *db/db* uninephrectomized (*db/db*-uni) mice, and treatment with the circulating soluble form of α-Klotho (cKL) reduces hyperphosphatemia: representative differences in histopathological changes in kidneys from lean mice (*A*, *C*, and *E*) and *db/db*-uni LacZ mice (*B*, *D*, and *F*). *A*: hematoxylin-eosin (H&E)-stained section with normal renal pelvis (RP) and absence of inflammation. *B*: H&E-stained section showing a dilated renal pelvis with focally extensive inflammatory infiltrate (black arrows) that extends into the transitional epithelial lining. *C*: Masson's trichrome (MTS)-stained section showing normal glomeruli with open capillary loops and normal mesangial matrix (stars). *D*: MTS-stained section depicting increased fibroplasia in glomeruli (increased blue matrix) with relative paucity of open capillary loops (yellow arrows). *Inset* shows a sclerotic glomerulus that has lost the normal glomerular architecture. Minimal interstitial fibrosis between the tubules is also highlighted in blue. *E*: periodic acid-Schiff (PAS)-stained section demonstrating normal mesangial matrix and open capillary loops (stars). *F*: significantly increased mesangial matrix deposition highlighted by PAS staining that frequently obliterates the normal capillary loops and cellularity in the glomeruli (yellow arrows). Glomeruli in *db/db*-uni LacZ mice are slightly larger than those in the lean mice because of functional hypertrophy subsequent to uninephrectomy. *G*: lean control (*db/dm*) mice were significantly lighter than all *db/db*-uni mice, regardless of albumin-to-creatinine ratio (ACR) or treatment group (**P* < 0.05). *H*: all *db/db*-uni mice, regardless of ACR or treatment group, had a lower heart weight-to-body weight (BW) ratio compared with lean controls (**P* < 0.05).

Fig. 2.

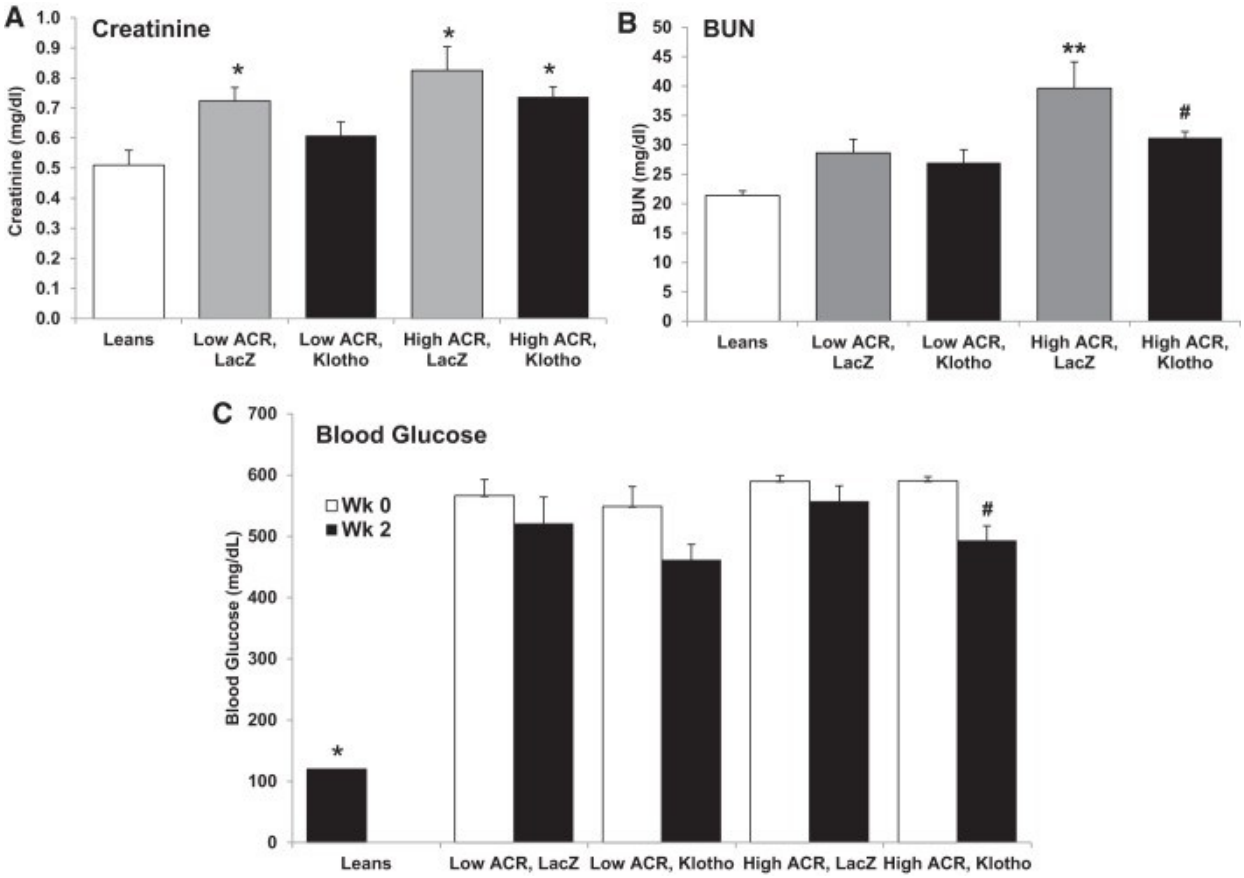

Administering adeno-associated virus 2/8 expressing the circulating soluble form of α-Klotho (AAV-cKL) to *db/db* uninephrectomized (*db/db*-uni) mice moderately improves kidney function and blood glucose. *A*: creatinine was elevated in low-albumin-to-creatinine ratio (ACR)/LacZ, high-ACR/LacZ, and high-ACR/cKL groups compared with lean controls (**P* < 0.05). *B*: blood urea nitrogen (BUN) was significantly higher in high ACR/LacZ (***P* < 0.01 vs. lean). AAV-cKL treatment reduced BUN after 6 wk (#*P* < 0.01 vs. high ACR/LacZ). *C*: blood glucose of lean control mice was significantly lower than that of all *db/db*-uni mice (**P* < 0.01). Two weeks of AAV-cKL treatment significantly reduced blood glucose values in the high-ACR/cKL group (#*P* < 0.05).

Fig. 3.

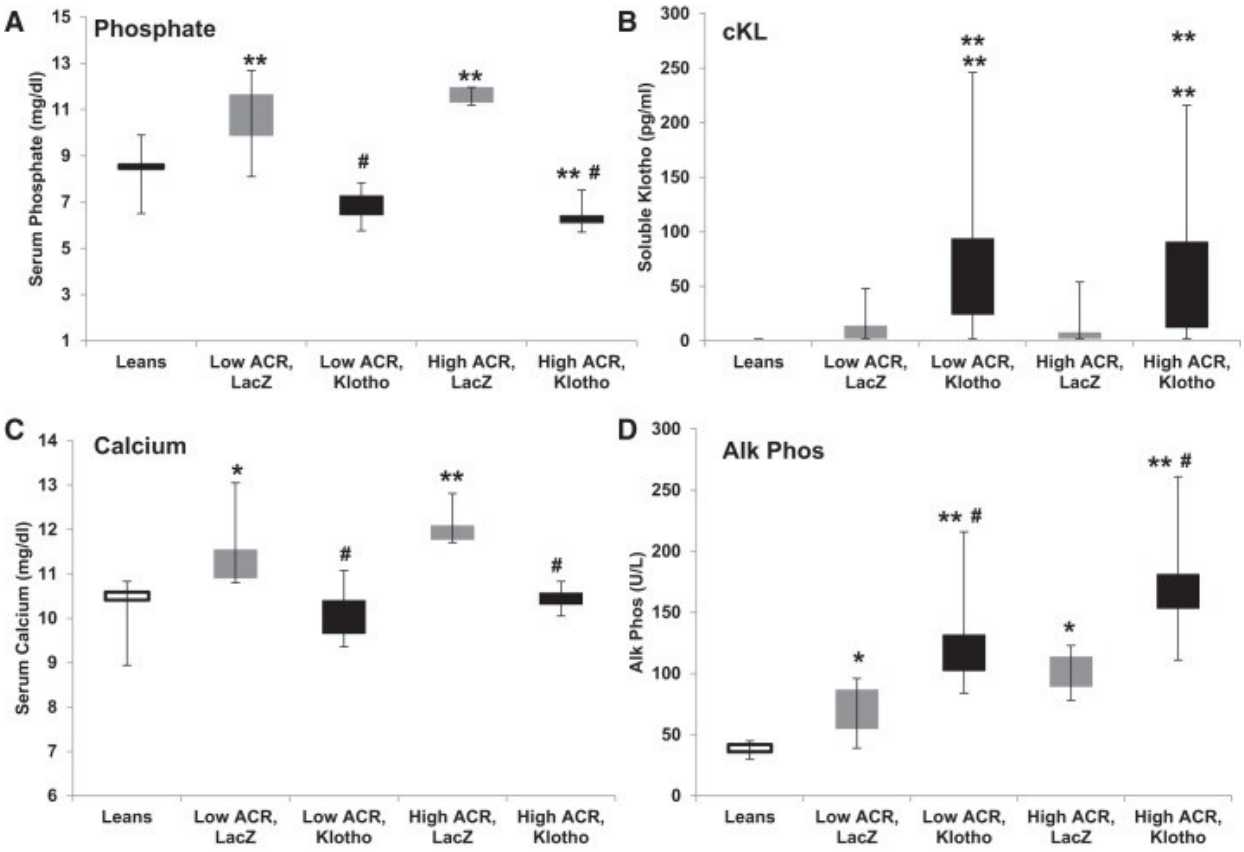

Endocrine effects of adeno-associated virus 2/8 expressing the circulating soluble form of α-Klotho (AAV-cKL) in lean and *db/db* uninephrectomized (*db/db*-uni) mice. *A*: *db/db*-uni mice in both the low- and high-albumin-to-creatinine ratio (ACR) groups were hyperphosphatemic (***P* < 0.01 vs. lean). Serum phosphate was significantly reduced in *db/db*-uni mice in both the low- and high-ACR groups 6 wk after AAV-cKL injection (#*P* < 0.01 vs. respective LacZ). AAV-cKL treatment in high-ACR *db/db*-uni mice significantly reduced serum phosphate compared with lean mice (***P* < 0.01). *B*: serum Klotho levels in *db/db*-uni mice were significantly increased with AAV-cKL treatment 6 wk postinjection (***P* < 0.01 vs. lean and respective LacZ). *C*: serum calcium was elevated in *db/db*-uni mice in both the low- and high-ACR groups treated with AAV-LacZ (**P* < 0.05 and ***P* < 0.01 vs. lean). AAV-cKL treatment reduced serum calcium in both the low- and high-ACR groups (#*P* < 0.05 vs. respective ACR/LacZ). *D*: *db/db*-uni mice, regardless of ACR group, have elevated serum alkaline phosphatase (Alk Phos; **P* < 0.05 and ***P* < 0.01 vs. lean). Treatment with AAV-cKL further elevated serum alkaline phosphatase in low- and high-ACR groups (#*P* < 0.05 vs. respective ACR/LacZ).

Fig. 4.

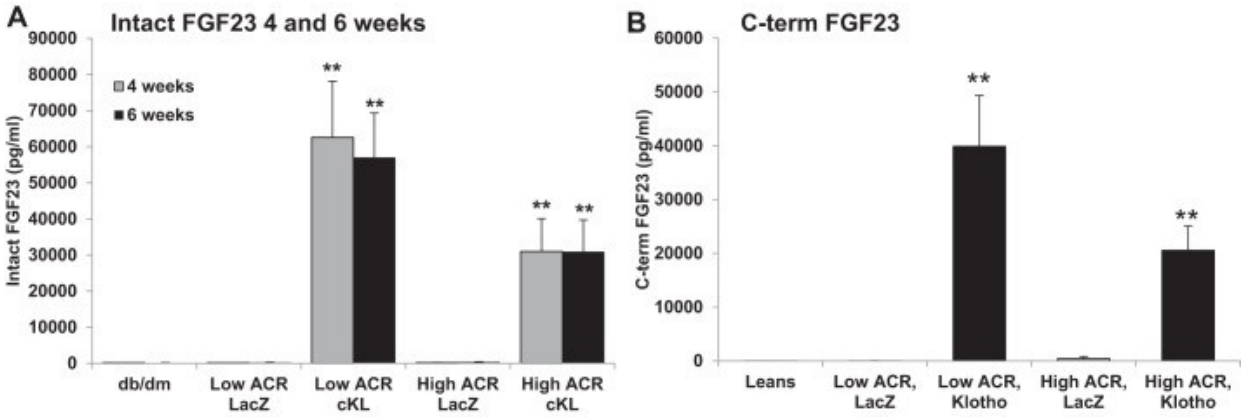

Changes in FGF23 processing with treatment with the circulating soluble form of α-Klotho (cKL) and downstream targets. *A*: intact FGF23 was significantly elevated in low- and high-albumin-to-creatinine ratio (ACR) groups of *db/db* uninephrectomized (*db/db*-uni) mice treated with adeno-associated virus 2/8 expressing cKL (AAV-cKL) at 4 and 6 wk postinjection (**$P < 0.01$). Six- and eight-week control values for intact FGF23 were as follows: *db/dm*: 133.8 ± 23.7 and 153.7 ± 8.2; low-ACR LacZ: 156.4 ± 25.2 and 233.5 ± 48.0; high-ACR LacZ: 209.0 ± 50.8 and 361.5 ± 102.5, respectively. *B*: COOH-terminal (C-term) fragments of FGF23 were significantly elevated in low- and high-ACR groups of *db/db*-uni mice treated with AAV-cKL at 4 and 6 wk postinjection (**$P < 0.01$). Control values for C-term FGF23 were as follows: *db/dm*: 1.1 ± 0.6; low-ACR LacZ: 29.9 ± 16.1; high-ACR LacZ: 415.5 ± 388.0.

Fig. 5.

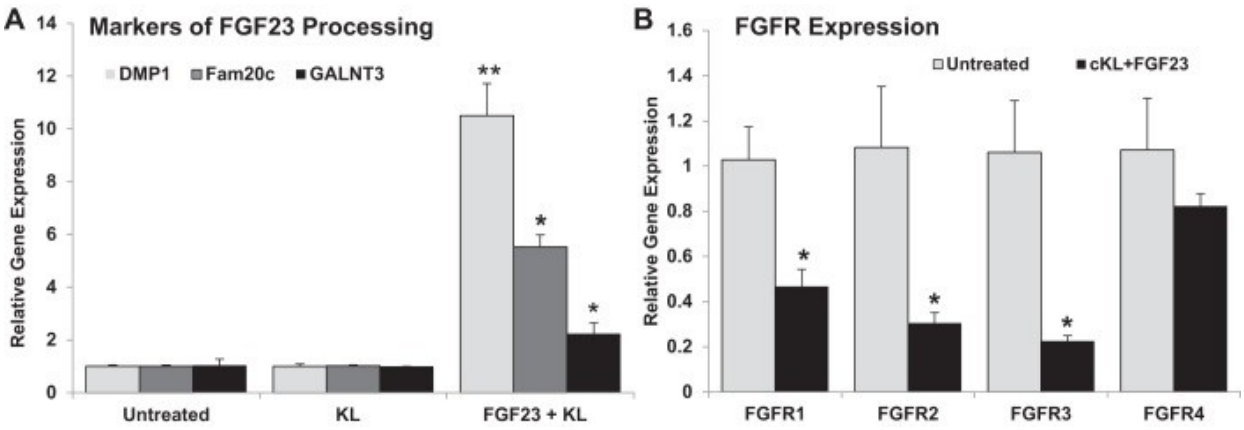

Changes in downstream targets of FGF23 signaling and FGF receptor (FGFR) expression with treatment with the circulating soluble form of α-Klotho (cKL). *A*: cKL and FGF23 combination treatment (FGF23 + KL) increased polypeptide *N*-acetylgalactosaminyltransferase 3 (GALNT3; **P* < 0.05), dentin matrix protein-1 (DMP1; ***P* < 0.01), and extracellular serine/threonine protein kinase FAM20C (FAM20C; **P* < 0.05) mRNA expression. cKL treatment alone (KL) had no effect on mRNA expression. *B*: FGFR1, FGFR2, and FGFR3 mRNA expression was significantly reduced by combination treatment of cKL and FGF23 (**P* < 0.05). FGFR4 mRNA expression was not statistically different from control following combination treatment.